Two-electron systems in strong laser fields

G. Camiolo,[1] G. Castiglia,[1] P. P. Corso,[1] E. Fiordilino,[1,*] and J. P. Marangos[2]

[1]*Dipartimento di Scienze Fisiche e Astronomiche and CNISM, Università di Palermo, Via Archirafi 36, 90123 Palermo, Italy*
[2]*Blackett Laboratory, Imperial College London, Prince Consort Road, South Kensington, London SW7 2AZ, United Kingdom*

In this paper we investigate the single and double ionization signals of H_2 molecules, with fixed and moving nuclei, as a function of laser intensity, for two different values of laser wavelength (λ=390 nm and λ=780 nm), using an approach for evaluating the ionization signals which allows the investigation of relatively long-lasting pulses. The He system is first investigated to benchmark our calculation against already known results. We confirm the evidence of nonsequentiality in the ionization processes of all the systems investigated. Furthermore, we show that the nuclei motion enhances the double ionization signals by means of a mechanism which is very similar to a charge-resonant enhanced ionization (CREI) effect [Zuo and Bandrauk, Phys. Rev. A **52**, R2511 (1995)].

I. INTRODUCTION

The interaction of a strong laser pulse of angular frequency ω_L with atoms and molecules gives the opportunity to observe processes which are nonlinear in the laser intensity and cannot be described by the standard perturbation theory. Among these processes we mention high-order harmonic generation (HHG) and nonsequential multiple ionization of atoms and molecules.

HHG consists of the emission by atoms and molecules of a wide plateau of harmonics of ω_L whose observed order can be much larger than N=100 [1]. Since the emitted power is proportional to the square modulus of the acceleration of the charges, the calculation of this quantity would require an accurate knowledge of the wave function of the electrons. Of course no realistic perturbative calculation can be used to describe such a phenomenon since it would require a treatment at least up to the Nth order. The response of atoms or molecules to the pumping field can be fruitfully described by assuming that only one of their electrons is active and responsible for the emission; this is the popular single active electron (SAE) approximation. Within SAE all electrons except one are considered frozen in their orbital and contribute to the dynamics through a static screening potential [2].

The laser field can ionize atoms and molecules and extraction of multiple electrons has been observed. The exact explanation of multiple ionization is generally the balance of various mechanisms: the crucial experimental point is that the yield for double ionization is very large and its magnitude cannot be obtained by simply considering the double extraction process as produced by two individually independent and sequential steps, which are two sequential SAE steps [3].

The outputs of the suggested, nonsequential, ionization models are rather similar and agree sufficiently well with the experiments although differ from their microscopic temporal evolution [4–13]. They can be loosely grouped into two main families: the first one (shake-off models [3]) assumes that the

extraction of one of the two electrons is such an abrupt process that the remnant electron does not have time to adapt to the new ionic potential and is left in an excited state from where it is extracted shortly later by the laser. The second family (rescattering models [14]) assumes that the first extracted electron is pushed by the same laser field, which in the meanwhile inverted its phase, back to the parent ion where after a collision scatters the second electron into the continuum. Actually this second mechanism is strongly dependent on the laser polarization; in fact, a circularly polarized field does not allow a return trajectory to the ion and so prevents the double ionization [5,15].

A different mechanism of double ionization can be related to the Auger effect. Here, after extraction of an inner electron, the atom, left in an autoionizing state, minimizes its energy by filling the vacancy with an outer electron; the decaying electron transfers its excess energy to an outer electron via Coulomb repulsion which is promoted to the continuum [16–18]. This mechanism, which cannot work for helium or light atoms, is effective in heavy atoms and molecules and requires the correlation of the two active electrons undergoing the transitions.

Experiments and theoretical curves of multiple ionization yields as a function of the laser intensity I_L present an initial power law shape of the type I_L^n that can be explained by a nth order perturbation regime followed by a *knee* flagging the breakdown of the perturbative approach. The challenge, set by the problem of multiple ionizations to the theorists, is related to the coupling of the difficulties of nonlinear processes with those of treating satisfactorily correlation effects [19]. The scenario becomes rather more complicated if the dissociation of the molecule during the laser operation is taken into consideration. The presence of the laser field induces oscillations of the electronic wave function [20,21] that result in a force acting on the nuclei thus activating molecular vibrations [22,23]. Since the electrons provide the only binding mechanism for the molecule, it is to be expected that electron extraction induces molecular dissociation.

Recently it has been suggested that the dynamics of molecules can be directly accessible to real-time observation by

*fiordili@fisica.unipa.it

detecting the harmonics diffused by the molecule acted upon by a laser field. The basic reason of this possibility is related to the fact that the acceleration of the charge that produces the harmonics is a quantity intrinsically determined by the physical environment where the charge is located; it is therefore to be expected that the generated field carries along with itself information on the location and behavior of the charge. Several simulations have shown that a measurement of the physical parameters characterizing the radiation improves the information that can be gained on the behavior of the charge [20,22,24,25]. Moreover a lot of current experimental activities on molecular HHG are motivated by the prospects of new types of ultrafast measurements of molecular structure [26,27]. Such approaches demand a much better understanding of the nuclear dynamics (which play a very important role in HHG [28]) and also require the multielectron part of the problem to be addressed as invariably molecular systems require a treatment beyond a SAE approach to be realistic. Our work addresses both these issues and the interplay between them, which is vital to a sound understanding of this important and current problem.

In this paper we study the single and double ionization signals for a simple molecular system, namely, H_2 molecule, investigating both fixed and moving nuclei systems, using strong-field (laser intensity on the order of 5×10^{15} W/cm^2) long-lasting [more than 20 optical cycles (o.c.)] laser pulses of different frequencies: $\lambda = 390$ nm and $\lambda = 780$ nm. In particular we show how the molecular dynamics, although mod-

est in absolute value, is responsible for a consistent modification of the single and double ionization yields.

Since the investigated pulses are long enough for allowing the electron wave function to reach the boundaries of the numerical box, we have introduced a theoretical and numerical approach for evaluating the ionization signals which does not suffer the limitations of most of the other previously developed methods. In order to check this approach, we apply it to a well-known system, the He atom. The results obtained for this atomic system are also used as a benchmark for a comparison with the corresponding results pertaining the H_2 molecule.

II. THEORY

In this section we introduce the formal treatment we use for investigating the dynamics of both He atom and H_2 molecule in the presence of a strong laser field.

Assuming that the laser is linearly polarized, since most of the electron and nuclei dynamics occur in the laser direction, we study a one-dimensional model for both the electrons and nuclei coordinates. In what follows R_1 and R_2 indicate the nuclei positions ($R_1 = R_2 = 0$ for He) and x_1 and x_2 indicate the electron positions; furthermore M and m indicate the nuclei and the electron masses, respectively, and $-e$ being the electron charge. The temporal evolution of such a system is described by the time-dependent Schrödinger equation (TDSE),

$$i\hbar \frac{\partial \Phi(R_1,R_2,x_1,x_2,t)}{\partial t} = \left[-\frac{\hbar^2}{2m}\left(\frac{\partial^2}{\partial x_1^2} + \frac{\partial^2}{\partial x_2^2} \right) - \frac{\hbar^2}{2M}\left(\frac{\partial^2}{\partial R_1^2} + \frac{\partial^2}{\partial R_2^2} \right) + U(R_1,R_2,x_1,x_2) + V(R_1,R_2,x_1,x_2,t) \right] \Phi(R_1,R_2,x_1,x_2,t),$$

$$(1)$$

where

$$U(R_1,R_2,x_1,x_2) = -\frac{e^2}{\sqrt{A+(x_1-R_1)^2}} - \frac{e^2}{\sqrt{A+(x_1-R_2)^2}} - \frac{e^2}{\sqrt{A+(x_2-R_1)^2}} - \frac{e^2}{\sqrt{A+(x_2-R_2)^2}} + \frac{e^2}{\sqrt{A_{12}+(x_1-x_2)^2}} + \frac{e^2}{\sqrt{A_N+(R_1-R_2)^2}}$$

$$(2)$$

is the potential energy of the system and

$$V(R_1,R_2,x_1,x_2,t) = e(-R_1-R_2+x_1+x_2)E_0 f(t)\sin(\omega_L t)$$

$$(3)$$

is the laser-molecule interaction energy in the dipole approximation, with E_0 as the peak laser electric field amplitude and $f(t)$ as the laser pulse profile.

As it is evident from Eq. (2) we use a soft-core potential [29] to model the electrostatic interactions among the electrons and the nuclei, the screening parameters A, A_{12}, and A_N being responsible for the softening of the interaction of the

electron-nuclei, electron-electron, and nucleus-nucleus interaction, respectively.

Of course the presence of both the electrons and the nuclei coordinates as quantum degrees of freedom makes it very difficult either the analytical or the numerical solution of the full Schrödinger equation [Eq. (1)]. In order to simplify the treatment of the system, it is possible to introduce some approximations which allow us to deal with only two quantum coordinates (the electron ones) and with two classical coordinates (the nuclei ones). This approximation relies on the evidence that the proton mass is much larger than the electron one, so we may assume that it is possible to decouple the nuclei dynamics from the electron dynamics; this is the well-known adiabatic approximation [30].
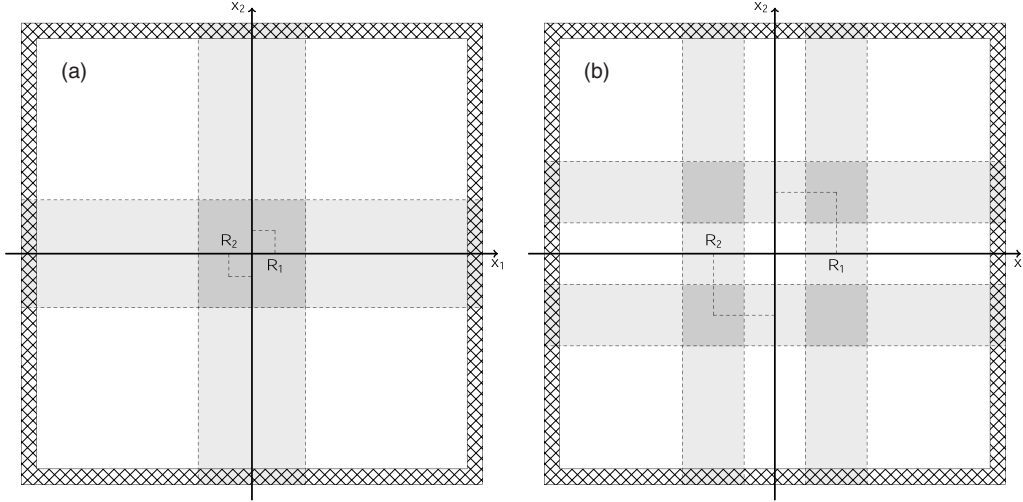
FIG. 1. Schematic plot of different ionization regions: dark gray for no-ion regions, gray for single-ion regions, and white for double-ion regions. (a) corresponds to a situation with the internuclear separation less than the no-ion region width [(b) $x_0 = 10$ a.u.] to the opposite situation.

With this assumption in mind [31] the time evolution of the system is obtained by a TDSE for the electron wave function

$$i\hbar \frac{\partial}{\partial t} \psi(x_1, x_2, t) = \hat{H}_e \psi(x_1, x_2, t), \qquad (4)$$

with $\psi(x_1, x_2, t)$ as the electronic wave function and

$$\hat{H}_e = -\frac{\hbar^2}{2m}\left(\frac{\partial^2}{\partial x_1^2} + \frac{\partial^2}{\partial x_2^2}\right) + U[R_1(t), R_2(t); x_1, x_2]$$
$$+ e(x_1 + x_2)E_0 f(t)\sin(\omega_L t), \qquad (5)$$

and by a set of two Newton equations for the instantaneous positions of the nuclei,

$$M\ddot{R}_1(t) = F_{12}(t) + F_{1e}(t) + F_L(t),$$

$$M\ddot{R}_2(t) = F_{21}(t) + F_{2e}(t) + F_L(t). \qquad (6)$$

In Eq. (5) the nuclear coordinates $R_1(t)$ and $R_2(t)$ must be considered given functions of time and are obtained by solving Eq. (6); $U[R_1(t), R_2(t); x_1, x_2]$ is numerically given by $U(R_1, R_2, x_1, x_2)$: in our notation a semicolon separates non-dynamical from dynamical variables. In Eq. (6), the nuclei electrostatic interaction $F_{12}(t)$ is

$$F_{12}(t) = e^2 \frac{R_1(t) - R_2(t)}{[A_N + |R_1(t) - R_2(t)|^2]^{3/2}}, \qquad (7)$$

with $F_{12}(t) = -F_{21}(t)$ and $F_L(t) = eE_0 f(t)\sin(\omega_L t)$ as the forces exerted by the laser on each nucleus. Finally the force exerted by the electrons on the nth nucleus is obtained by quantum averaging the softened Coulomb force over the electron wave function

$$F_{ne}(t) = -e^2 \int\int \frac{[R_n(t) - x_1]|\psi(x_1, x_2, t)|^2}{\{A + [R_n(t) - x_1]^2\}^{3/2}} dx_1 dx_2$$
$$- e^2 \int\int \frac{[R_n(t) - x_2]|\psi(x_1, x_2, t)|^2}{\{A + [R_n(t) - x_2]^2\}^{3/2}} dx_1 dx_2, \quad n = (1, 2).$$
$$(8)$$

Equations (4) and (6) must be solved simultaneously, starting from opportunely chosen initial values for the nuclei positions $R_n(t_0)$ ($n = 1, 2$) and for the electrons wave function $\psi(x_1, x_2, t_0)$, evaluated at the initial time t_0. This method was suggested in [32] for the case of the H_2^+ and fruitfully used in [21–23].

III. FIXED-NUCLEI RESULTS

A. Bare systems

After having introduced the general formalism for the system at hand, we now focus on the particular case of nuclei fixed at the positions R_1 and R_2. The dynamics of the molecule is strongly influenced by the eigenstate symmetry properties and to show it we need to introduce some properties of the bare molecule which now is described by the bare Hamiltonian

$$\hat{H}_e^B(R_1, R_2; x_1, x_2) = -\frac{\hbar^2}{2m}\left(\frac{\partial^2}{\partial x_1^2} + \frac{\partial^2}{\partial x_2^2}\right) + U(R_1, R_2; x_1, x_2),$$
$$(9)$$

where R_1 and R_2 must be considered fixed parameters, being the electron coordinates x_1 and x_2 the only dynamical variables. The potential energy term U, appearing in Eq. (9) and defined in Eq. (2), explicitly contains a contribution for the nuclei-nuclei electrostatic repulsion, namely, $e^2/\sqrt{A_N + R^2}$, with $R = |R_1 - R_2|$ being the internuclear distance. Such a term may be considered simply a shift in the energy levels of the bare system since it does not depend on any dynamical vari-

able; it is taken into account in order to obtain the correct total energies of the system and used in what follows to find the equilibrium position of the system itself.

The eigenstates and eigenenergies are found by numerically solving the TDSE

$$\hat{H}_e^B(R_1,R_2;x_1,x_2)u(R_1,R_2;x_1,x_2) = E(R)u(R_1,R_2;x_1,x_2)$$

(10)

by means of a recursive imaginary time propagation algorithm [33] with the parity of the eigenfunctions taken into account. For more information on the method of solution the interested reader is referred to [21].

In order to deal with a specific system we fix the screening parameters, the qualitative description of the system being roughly independent from their exact value: the best practice is to choose them to reproduce some of the relevant parameters of the real system. In what follows, in order to deal with as few arbitrary parameters as possible, we set $A_N=0.03a_0^2$ and $A=A_{12}\equiv1a_0^2$, with a_0 being the Bohr radius. With such a choice of the relevant parameters, we obtain for He a ground state energy of $E_g^{He}=-2.24e^2/a_0$ and for H_2 an equilibrium internuclear separation of $R_0=2.13a_0$ and a ground state energy of $E_g^{H_2}=-1.39e^2/a_0$. For comparison we mention that the values for the real He and H_2 molecule are $E_g^{He}=-2.90e^2/a_0$, $R_0=1.4a_0$ and $E_g^{H_2}=-1.16e^2/a_0$, respectively. Although the parameters of the model system do not match exactly those of the real system the model does capture essential aspects of the physical system [34].

B. Laser driven systems

We are now ready to focus on the results concerning the dynamics of both He atom and H_2 molecule, initially in their ground state, interacting with a linearly polarized laser field of wavelength $\lambda=390$ nm or $\lambda=780$ nm in the range of laser intensity $I_L=10^{14}-4\times10^{15}$ W/cm^2.

We start investigating the dynamics of both He atom and H_2 molecule with fixed nuclei. In order to study such dynamics, we solve numerically only Eq. (4) by using a split operator method [35] in a two-dimensional spatial box in the range $[-b,b]$ with $b=256a_0$ using a spatial step $\Delta x=a_0/4$ and a temporal step which depends on the laser intensity. In order to avoid reflection of the wave function at the boundary of the integration spatial box we use a sin^2 absorbing mask acting on a spatial box $b/10$ wide. In what follows, we mainly focus our attention on the study of the electron ionization signals as a function of either the internuclear distance R or the laser intensity I_L. A very simple method to measure the various electron ionization signals is obtained by introducing a distance parameter x_0 [36–38], which settles a criterion of electron proximity to the nuclei; we have chosen $x_0=10a_0$. The ith $(i=1,2)$ electron is considered not ionized if either the condition $|x_i-R_1|\le x_0$ or $|x_i-R_2|\le x_0$ ($i=1,2$) (or both) is satisfied. For a H_2 molecule (He atom is considered a special case of H_2 molecule with $R=0$) it is thus possible to define three regions in our integration box, one for each of the possible electron ionization states:

(i) not-ionized region when both electrons are within x_0 of one or both the nuclei;

(ii) single-ionized region if one of the electron is within x_0 one of the nuclei and the other electron is further away; and

(iii) double-ionized region if both electrons are more than x_0 away from both the nuclei.

In Fig. 1 we show two different schemes for the ionization regions; Fig. 1(a) corresponds to the case in which $R<x_0$ and Fig. 1(b) to case in which $R>x_0$. Dark gray indicates the not-ionized electron regions, gray indicates the single-ionized electron regions, and white indicates the double-ionized electron regions. Figure 1(a) describes most of the cases for real molecules; nevertheless Fig. 1(b) is usually appropriate when molecular dissociation can occur.

In order to evaluate the single and double ionization signals, especially for long-lasting laser pulses, it is not possible to integrate $|\psi(x_1,x_2,t)|^2$ over the above mentioned three regions since part of the electronic density has been already *absorbed* by the mask. The contribution of the absorbed wave function to the ionization signals could be obtained by cumulating the fluxes of the electron density current through the boundaries of the various ionization regions, as shown in [39]; nevertheless this approach requires the numerical determination of spatial derivatives and introduces large errors particularly significant when a strong laser is acting.

In this paper we suggest a different method to evaluate the ionization signals which allows us to overcome the above mentioned problems: we take into account the wave function distributed in the various inner regions of the integration spatial box plus the wave function portions absorbed by the mask as contributing to the ionization signals corresponding to the various regions of the spatial box. This technique does not require the evaluation of additional quantities, such as derivatives, which could introduce errors, and preserves the total norm (no-ion signal plus single-ion signal plus double-ion signal) equal to one. Obviously, the edge of the wave function in reaching the absorbing region disappears and cannot migrate to other ionization regions. The adoption of a large integration box ($512a_0$ wide) makes unlikely, in the far away region, population exchange among the different ionization areas.

We start by studying single and double ionization signals for He atom and H_2 molecule with fixed nuclei as a function of laser intensity. We always assume the laser pulse shape to be trapezoidal, with 2 o.c. of turn-on and turn-off and various constant pulse region durations. Furthermore we add at the end of the trapezoidal pulse 2 o.c. of free propagation in order to be sure about the stability of the obtained results. In Fig. 2 we show the ionization signals of He for laser wavelength $\lambda=780$ nm and different total durations of the pulse: (a) 8, (b) 10, (c) 14, and d) 22 o.c. In the insets of the various plots of this figure we show the ratio of the results corresponding to $\lambda=390$ nm and the present results with $\lambda=780$ nm. The ionization signals of He$^+$ are also shown for the sake of comparison. From all these plots it is evident the presence of the typical knee structure in the double ionization signal, which is in agreement with the experimental measurement of the ionization signals from small molecules and differs from SAE model predictions [40]. At large laser intensity the double ionization signal becomes comparable to
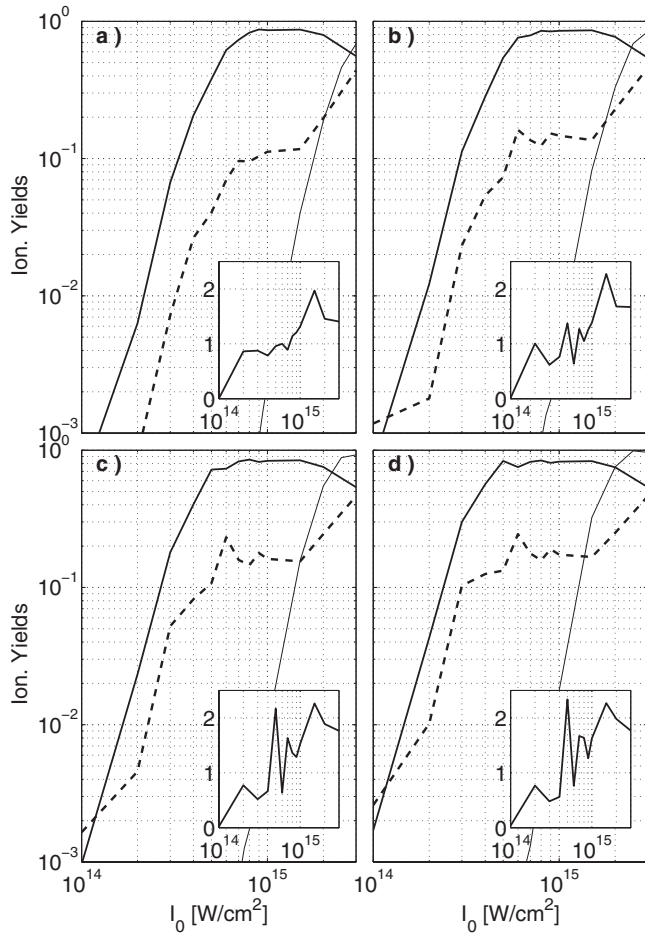
FIG. 2. Single (thick continuous lines) and double (dashed lines) ionization signals for He atom and laser wavelength of 780 nm for different pulse durations: (a) $T=8$ o.c., (b) $T=10$ o.c., (c) $T=14$ o.c., and (d) $T=22$ o.c. Thin continuous lines show the He$^+$ ionization signals used as a benchmark for showing the nonsequentiality of the double ionization signals. In the insets we plot the ratio between the double ionization signals obtained for $\lambda=390$ nm and those for $\lambda=780$ nm.

FIG. 3. Single (thick continuous lines) and double (dashed lines) ionization signals for H$_2$ molecule with fixed nuclei and laser wavelength 390 nm for different pulse durations: (a) $T=8$ o.c., (b) $T=10$ o.c., (c) $T=14$ o.c., and (d) $T=22$ o.c. Thin continuous lines show the He$^+$ ionization signals used as a benchmark for showing the nonsequentiality of the double ionization signals.

$$\Lambda = \frac{eE_0}{m\omega_L^2} \tag{11}$$

the ionization signal of He$^+$; this feature is generally regarded as marking the onset of the sequential double ionization: the laser is indeed strong enough to extract both the electrons regardless of their correlation. It appears that the nonsequentiality of the double ionization signal is strongly related to the pulse duration; in particular the characteristic knee structure becomes more and more defined as we increase the pulse duration. Furthermore, it is evident that the laser wavelength is another critical parameter in determining the details of the nonsequentiality of the ionization; the double ionization signals, for intensities in the knee region and above, are higher for $\lambda=390$ nm than for $\lambda=780$ nm, as shown in each inset in Fig. 2 plotting the ratio of the double ionization signals for $\lambda=390$ nm and $\lambda=780$ nm. Presumably, for a laser intensity below 10^{15} W/cm^2, this is due to the fact that, for a given laser intensity, the shorter wavelength, corresponding to lower ponderomotive energies, is responsible for a smaller electron excursion
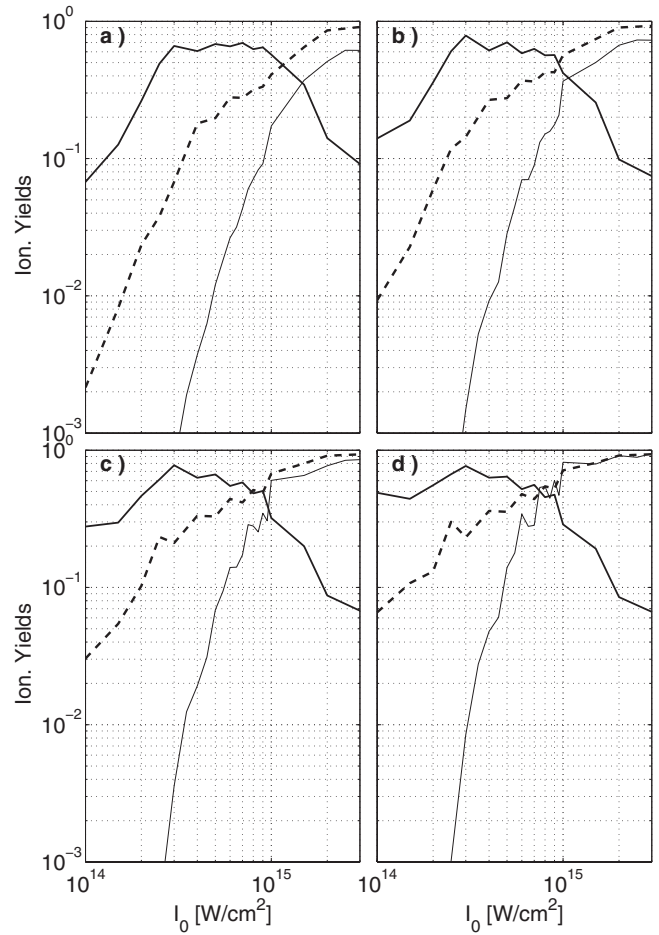
around the nuclei, thus allowing higher electron-electron interaction which contributes to nonsequential double ionization signal.

Results similar to those just described for He atom are obtained for the ionization yields of the fixed nuclei H$_2$ molecular model as shown in Figs. 3 and 4. These yields have been obtained starting from the ground state of the H$_2$ at the equilibrium distance ($R_0=2.13a_0$). The main difference between these results and those for He consists of the heights of the double ionization yields; in particular they appear to be higher for H$_2$ than for He. We think this result is due to the lower ionization energy of the ground state of H$_2$ with respect to the ground state of He.

From the previous plots it appears that the nonsequential double ionization mechanism dominates in the region $I_0 \lesssim 10^{15}$ W/cm^2. Nevertheless a detailed study of the time evolution of the ionization signal casts light on the phenomenon. In Fig. 5 we plot the ionization signals (both single and
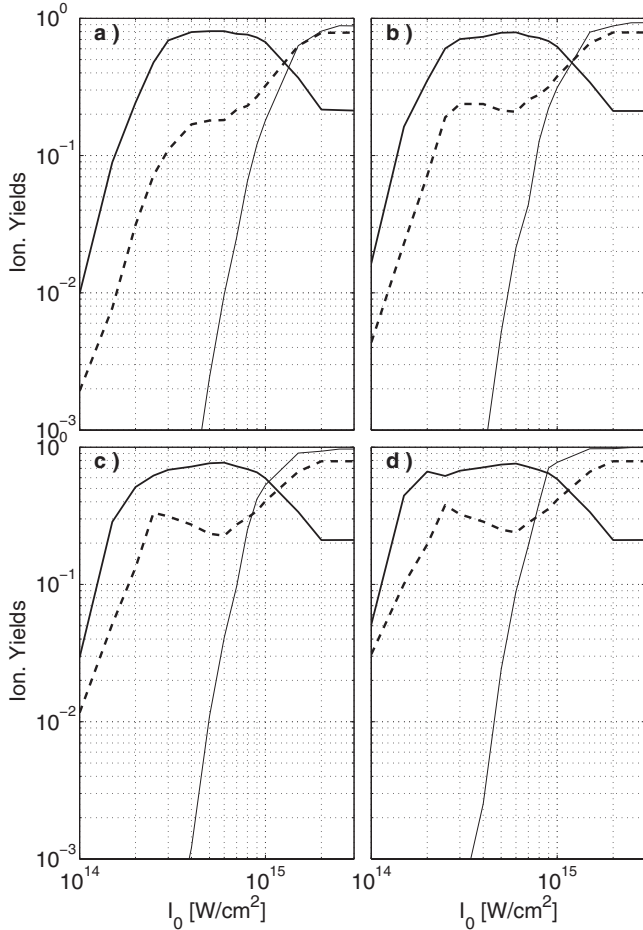
FIG. 4. Single (thick continuous lines) and double (dashed lines) ionization signals for H_2 molecule with fixed nuclei and laser wavelength of 780 nm for different pulse durations: (a) $T=8$ o.c., (b) $T=10$ o.c., (c) $T=14$ o.c., and (d) $T=22$ o.c. Thin continuous lines show the He^+ ionization signals used as a benchmark for showing the nonsequentiality of the double ionization signals.
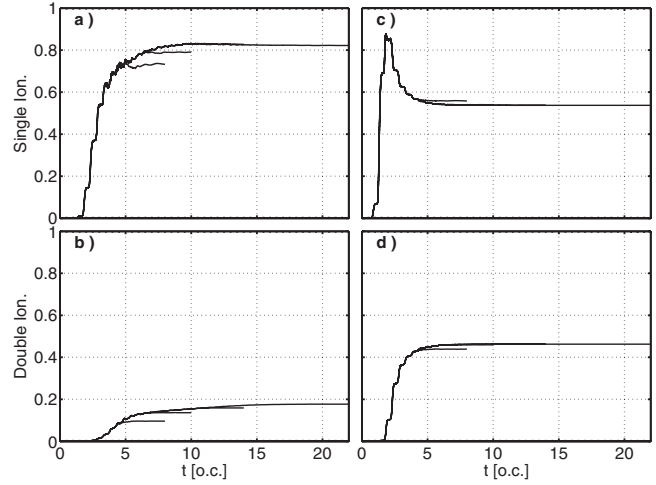

FIG. 5. Plots of single and double ionization signals for He atom subjected to laser of wavelength $\lambda=780$ nm and intensities $I_0=7 \times 10^{14}$ W/cm^2 [subplots (a) and b)] and $I_0=30\times10^{14}$ W/cm^2 [subplots (c) and (d)]. Any subplot shows four curves for different pulse durations (8, 10, 14, and 22 o.c.). The curves generally overlap.

double) of He as a function of time with $\lambda=780$ nm and for two different laser intensities, $I_0=7\times10^{14}$ W/cm^2 [subplots (a) and (b)] and $I_0=30\times10^{14}$ W/cm^2 [subplots (c) and (d)].

Since the lowest intensity, $I_0=7\times10^{14}$ W/cm^2, is within the nonsequential region, subplots (a) and (b) of Fig. 5 show that both single and double ionization signals increase with time until saturation at different values, depending on the pulse duration. A completely different behavior is observable in subplots (c) and (d) of Fig. 5 for the highest intensity, $I_0=30\times10^{14}$ W/cm^2, which lies in the sequential region; the single ionization signal starts increasing almost immediately during the turn-on of the pulse and reaches it maximum value ($\approx90\%$) at 2 o.c., with the double ionization signal almost absent. After that, the double ionization signal starts increasing at the expenses of the single ionization signal. This behavior is typical of sequential ionization: at the beginning of the laser pulse and for a short duration the emission of just one electron is relevant (the single ionization signal is relevant); after that the double ionization signal starts increasing, becoming soon the dominant signal.

Similar results are evident for the H_2 molecule with fixed nuclei, whose ionization signals as a function of time are

shown in Fig. 6 for $\lambda=780$ nm and $I_0=5\times10^{14}$ W/cm^2 [subplots (a) and (b)] and $I_0=20\times10^{14}$ W/cm^2 [subplots (c) and (d)].

IV. MOVING-NUCLEI RESULTS

The general approach introduced in Sec. II allows us to investigate the moving nuclei system, looking for the effects related to the dynamics of the nuclei in terms of both single and double ionization signals.

In Figs. 7 and 8 we show the ionization yields vs the laser intensity for two different wavelengths, $\lambda=390$ nm and
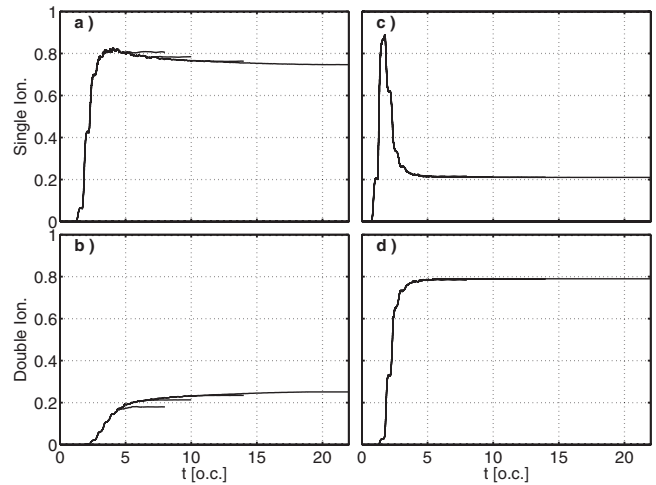

FIG. 6. Plots of single and double ionization signals for H_2 molecule with fixed nuclei subjected to laser of wavelength $\lambda=780$ nm and intensities $I_0=5\times10^{14}$ W/cm^2 [subplots (a) and (b)] and $I_0=20\times10^{14}$ W/cm^2 [subplots (c) and (d)]. Any subplot shows four curves for different pulse durations (8, 10, 14, and 22 o.c.). The curves generally overlap.
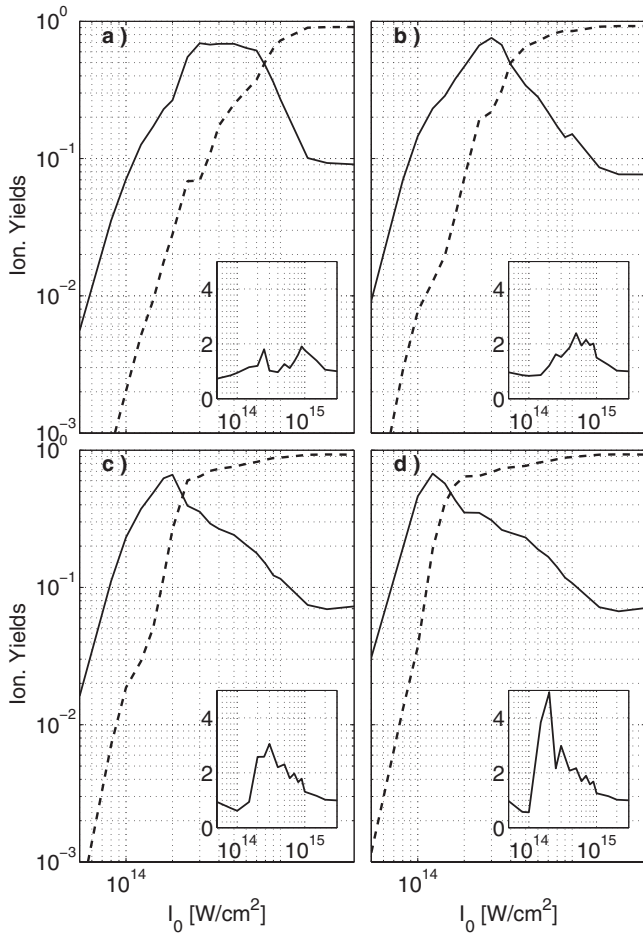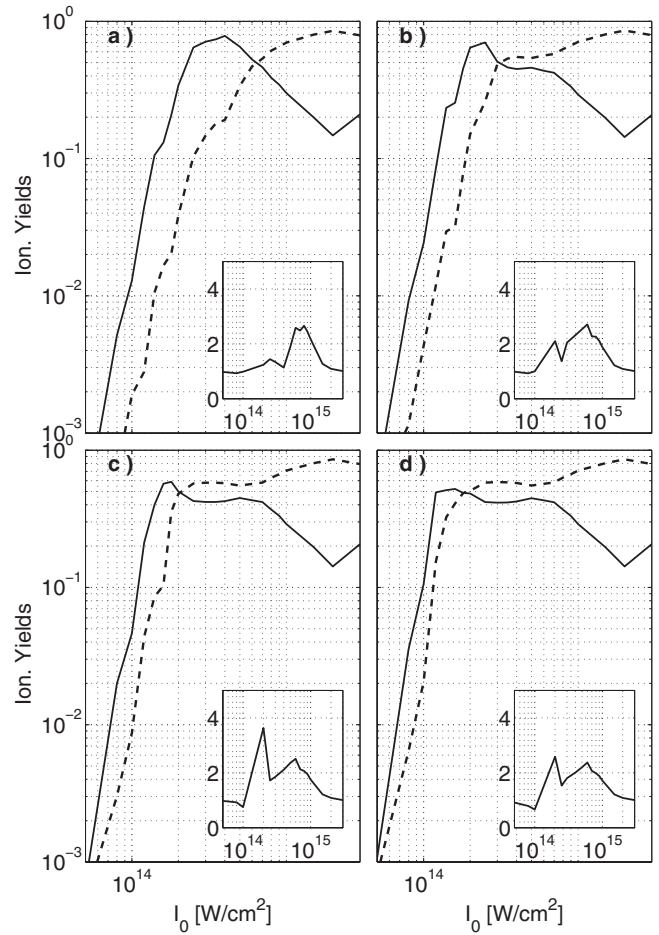
FIG. 7. Single and double ionization yields of H_2 molecule with moving nuclei, subjected to a laser whose wavelength is λ =390 nm, for different pulse durations: (a) T=6 o.c., (b) T =8 o.c., (c) T=12 o.c., and (d) T=20 o.c. The inset in each subplot shows the ratio of the double ionization yields of H_2 with moving nuclei versus H_2 with fixed nuclei.

FIG. 8. Single and double ionization yields of H_2 molecule with moving nuclei, subjected to a laser whose wavelength is λ =780 nm, for different pulse durations: (a) T=6 o.c., (b) T =8 o.c., (c) T=12 o.c., and (d) T=20 o.c. The inset in each subplot shows the ratio of the double ionization yields of H_2 with moving nuclei versus H_2 with fixed nuclei.

λ=780 nm, respectively, for H_2 molecule with moving nuclei. The inset of each subplot shows the ratio of the double ionization yield just plotted for moving nuclei molecule and the double ionization yield for the corresponding fixed nuclei molecule. The fact that these ratios are always greater than 1 (sometimes even greater than 2) means that the motion of the nuclei is responsible for the increase in the corresponding double ionization yield mainly in the low intensity region. It is interesting to observe how such an effect is evident also for pulses which last in total only few femtoseconds; this means that small nuclei vibrations are responsible for evident effects in terms of ionization signals.

In order to explain this phenomenon, we investigate the single and double ionization yields as a function of the (fixed) internuclear distance for different values of the laser intensity.

In Fig. 9 we plot the single and double ionization yields as a function of R for the H_2 molecule subjected to a laser whose wavelength is λ=780 nm and whose intensity is I_0 =5×10^{14} W/cm^2, and total pulse duration T=20 o.c. (for different pulse durations, laser wavelengths, and laser intensities the results are basically the same).
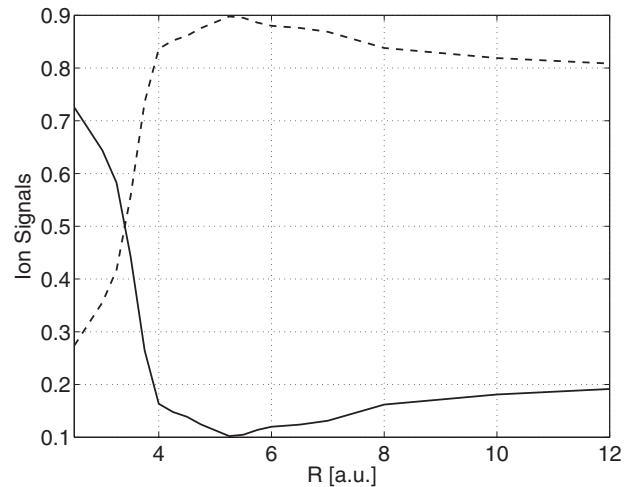

FIG. 9. Single (continuous line) and double (dashed line) ionization yields of H_2 molecule with fixed nuclei for different values of the internuclear distance R. The laser wavelength is λ=780 nm and the laser intensity is I_0=5×10^{14} W/cm^2.

Figure 9 shows a very interesting behavior of the ionization yields as a function of R. Close to the equilibrium position (in our simulation $R_0 = 2.13 a_0$), for the actual value of the laser intensity, the single ionization signal is higher than the corresponding double ionization signal; as R increases, it is evident a decreasing trend of the single ionization signal and a corresponding increasing trend of the double ionization signal until $R \simeq 5.5 a_0$ for which the double ionization signal reaches its maximum value of 0.9 and the single ionization signal reaches its minimum value of 0.1. This means that the H_2 molecule experiences a sort of charge-resonant enhanced ionization (CREI) effect [41] regarding the double ionization signal profile with a maximum at an internuclear distance considerably higher than the equilibrium distance.

Having this picture in mind, it is possible to give an explanation of the enhancement of the double ionization signal of H_2 with moving nuclei with respect to H_2 with fixed nuclei. As the nuclei move (basically either vibrating or exploding) they let the electrons explore different configurations which are associated to higher ionization yields with respect to the initial configuration, thus increasing the overall double ionization signal.

V. FINAL REMARKS AND CONCLUSIONS

In this paper within a one-dimensional model we have carried out a systematic and detailed investigation of the single and double ionization yields of H_2 and He and as a function of laser intensity and pulse duration and for two different laser wavelengths: $\lambda = 390$ nm and $\lambda = 780$ nm. To take into account strong fields ($I_L = 10^{15}$ W/cm^2) and long-lasting pulses (20 o.c.) we have introduced an approach for calculating the ion yields based on the cumulation of the electronic wave function absorbed by the mask.

Accordingly to all our results, the double ionization yield dominates the (full) ionization yield of the corresponding ion for lower values of I_L. This characteristic indicates that the process of extraction of two electrons is preferred to the extraction of one electron and should be read as a signature of a nonsequential mechanism for the double ionization act when this occurs.

We have shown that longer pulses extend and better define the knee structure present in the double ionization yield of He and H_2 with fixed nuclei. This result is compatible with the idea that the knee originates from the nonlinear electron-electron interaction.

The knee structure is also affected by the laser frequency; in particular, lower frequencies are responsible for smaller double ionization signals in the knee region. A physical interpretation of such a result is obtained by thinking that non-sequential double ionization is a result of the correlation and interaction between the two active electrons. The correlation is mostly effective when the laser induced quiver motion Λ is sufficiently small to allow strong interactions between the electron pair; this occurs at low intensity and high frequency of the driving field. A strong laser field completely dominates the electron dynamics thus overwhelming the electron correlation.

We have also characterized the nature of the ionization processes (sequential or nonsequential) in terms of the time profile of single and double ionization signals.

Finally we have investigated, by means of a semiclassical model, the effects of the dynamics of the nuclei for H_2 molecule on the ion yields. What we observed is a systematic increase in the double ionization signals for the moving nuclei cases. Such a phenomenon has been explained in terms of CREI effect.

ACKNOWLEDGMENTS

[1] A. L'Huillier and Ph. Balcou, Phys. Rev. Lett. **70**, 774 (1993).

[2] J. C. Slater, *Quantum Theory of Atomic Structure* (McGraw-Hill, New York, 1960), Vol. 1, Chap. 15.

[3] D. N. Fittinghoff, P. R. Bolton, B. Chang, and K. C. Kulander, Phys. Rev. Lett. **69**, 2642 (1992).

[4] B. Walker, B. Sheehy, L. F. Di Mauro, P. Agostini, K. J. Schafer, and K. C. Kulander, Phys. Rev. Lett. **73**, 1227 (1994).

[5] Th. Weber, H. Giessen, M. Weckenbrock, G. Urbasch, A. Staudte, L. Spielberger, O. Jagutzki, V. Mergel, M. Vollmer, and R. Dörner, Nature (London) **405**, 658 (2000).

[6] H. W. van der Hart and K. Burnett, Phys. Rev. A **62**, 013407 (2000).

[7] M. Lein, E. K. U. Gross, and V. Engel, Phys. Rev. Lett. **85**, 4707 (2000).

[8] A. Becker and F. H. M. Faisal, Phys. Rev. Lett. **89**, 193003 (2002).

[9] C. Figueira de Morisson Faria, H. Schomerus, X. Liu, and W. Becker, Phys. Rev. A **69**, 043405 (2004).

[10] M. Dörr, Opt. Express **6**, 111 (2000).

[11] J. L. Chaloupka, R. Lafon, L. F. Di Mauro, P. Agostini, and K. C. Kulander, Opt. Express **8**, 352 (2001).

[12] M. Lein, V. Engel, and E. K. U. Gross, Opt. Express **8**, 411 (2001).

[13] R. Moshammer, J. Ullrich, B. Feuerstein, D. Fischer, A. Dorn, C. D. Schröter, J. R. Crespo López-Urrutia, C. Höhr, H. Rottke, C. Trump, M. Wittmann, G. Korn, K. Hoffmann, and W.

Sandner, J. Phys. B **36**, L113 (2003).

[14] P. B. Corkum, Phys. Rev. Lett. **71**, 1994 (1993).

[15] D. N. Fittinghoff, P. R. Bolton, B. Chang, and K. C. Kulander, Phys. Rev. A **49**, 2174 (1994).

[16] G. Wentzel, Z. Phys. **43**, 524 (1927).

[17] D. Chatterji, *The Theory of Auger Transitions* (Academic, New York, 1976).

[18] E. Fiordilino, R. Zangara, and G. Ferrante, Phys. Rev. A **38**, 4369 (1988).

[19] W.-C. Liu, J. H. Eberly, S. L. Haan, and R. Grobe, Phys. Rev. Lett. **83**, 520 (1999).

[20] G. Castiglia, P. P. Corso, R. Daniele, E. Fiordilino, F. Morales, and F. Persico, J. Mod. Opt. **51**, 1163 (2004).

[21] R. Daniele, G. Camiolo, G. Castiglia, P. P. Corso, F. Morales, and E. Fiordilino, Appl. Phys. B: Lasers Opt. **78**, 813 (2004).

[22] P. P. Corso, R. Daniele, E. Fiordilino, J. P. Marangos, F. Morales, and R. Velotta, Phys. Rev. A **70**, 053410 (2004).

[23] G. Castiglia, G. Camiolo, P. P. Corso, R. Daniele, E. Fiordilino, and F. Morales, Laser Phys. **14**, 1185 (2004).

[24] E. Fiordilino, R. Daniele, and F. Morales, J. Phys. B **36**, 373 (2003).

[25] P. P. Corso, E. Fiordilino, and F. Persico, J. Phys. B **40**, 1383 (2007).

[26] J. Itatani, J. Levesque, D. Zeidler, H. Niikura, H. Pépin, J. C. Kieffer, P. B. Corkum, and D. M. Villeneuve, Nature (London) **432**, 867 (2004).

[27] N. L. Wagner, A. Wüest, I. P. Christov, T. Popmintchev, X. Zhou, M. M. Murnane, and H. C. Kapteyn, Proc. Natl. Acad. Sci. U.S.A. **103**, 13279 (2006).

[28] S. Baker, J. S. Robinson, C. A. Haworth, H. Teng, R. A. Smith, C. C. Chirilă, M. Lein, J. W. G. Tisch, and J. P. Marangos, Science **312**, 424 (2006).

[29] J. Javanainen, J. H. Eberly, and Q. Su, Phys. Rev. A **38**, 3430 (1988).

[30] M. Weissbluth, *Atoms and Molecules* (Academic, New York, 1978).

[31] M. Lein, Phys. Rev. Lett. **94**, 053004 (2005).

[32] B. Rotenberg, R. Taïeb, V. Veniard, and A. Maquet, J. Phys. B **35**, L397 (2002).

[33] R. Grobe and J. H. Eberly, Phys. Rev. A **48**, 4664 (1993).

[34] J. C. Slater, *Quantum Theory of Molecules and Solids* (McGraw-Hill, New York, 1963), Vol. 1.

[35] M. D. Feit and A. Steiger, J. Comput. Phys. **47**, 412 (1982).

[36] J. S. Parker, E. S. Smyth, and K. T. Taylor, J. Phys. B **31**, L571 (1998).

[37] H. G. Muller, Opt. Express **8**, 417 (2001).

[38] R. Panfili and W.-C. Liu, Phys. Rev. A **67**, 043402 (2003).

[39] M. Lein, E. K. U. Gross, and V. Engel, J. Phys. B **33**, 433 (2000).

[40] C. Cornaggia and Ph. Hering, Phys. Rev. A **62**, 023403 (2000).

[41] T. Zuo and A. D. Bandrauk, Phys. Rev. A **52**, R2511 (1995).